Amino Acids (2015) 47:2483–2493
DOI 10.1007/s00726-015-2033-y

ORIGINAL ARTICLE

A comparative study for adsorption of lysozyme from aqueous samples onto Fe_3O_4 magnetic nanoparticles using different ionic liquids as modifier

Sedigheh Kamran[1,2] · Ghodratollah Absalan[1] · Mozaffar Asadi[1]

Received: 5 January 2015 / Accepted: 16 June 2015 / Published online: 7 July 2015

Abstract In this paper, nanoparticles of Fe_3O_4 as well as their modified forms with different ionic liquids (IL–Fe_3O_4) were prepared and used for adsorption of lysozyme. The mean size and the surface morphology of the nanoparticles were characterized by TEM, XRD and FTIR techniques. Adsorption studies of lysozyme were performed under different experimental conditions in batch system on different modified magnetic nanoparticles such as, lysozyme concentration, pH of the solution, and contact time. Experimental results were obtained under the optimum operational conditions of pH 9.0 and a contact time of 10 min when initial protein concentrations of 0.05–2.0 mg mL^{-1} were used. The isotherm evaluations revealed that the Langmuir model attained better fits to the equilibrium data than the Freundlich model. The maximum obtained adsorption capacities were 370.4, 400.0 500.0 and 526.3 mg of lysozyme for adsorption onto Fe_3O_4 and modified magnetic nanoparticles by [C_4MIM][Br], [C_6MIM][Br] and [C_8MIM][Br] per gram of adsorbent, respectively. The Langmuir adsorption constants were 0.004, 0.019, 0.024 and 0.012 L mg^{-1} for adsorptions of lysozyme onto Fe_3O_4 and modified magnetic nanoparticles by [C_4MIM][Br], [C_6MIM][Br] and [C_8MIM][Br], respectively. The adsorption capacity of lysozyme was found to be dependent on its chemical structure, pH of the solution, temperature and type of ionic liquid as modifier. The applicability of two kinetic models including pseudo-first order and pseudo-second order model was estimated. Furthermore, the thermodynamic parameters were calculated. Protein could desorb from IL–Fe_3O_4 nanoparticles by using NaCl solution at pH 9.5 and was reused.

Keywords Magnetic nanoparticle · Ionic liquid · Adsorption · Lysozyme

Introduction

Magnetic nanomaterials have great promise in the design of electronic and electrical devices (Murray et al. 1995), separation methods (Altintas and Denizli 2009), biomedical applications (Roath 1993), tumor hyperthermia (Mornet et al. 2004) radioactive therapies (Widder et al. 1979; Gupta et al. 1988) and magnetic field-guided carriers for localizing drugs. The quantitative analysis of protein is of great importance in biochemistry, biotechnology, medical diagnostics and clinical application as it can provide information for diagnosis of diseases and measurement of other components. There are many methods for protein determination, such as spectrophotometry (Miao–Miao et al. 2011), fluorometry (Ghali 2010), and chemiluminescence (Li et al. 1998). At present, light scattering technique has been developed rapidly, especially in the determination of biological macromolecules, e.g., nucleic acid, proteins and glycogen (Parhi et al. 2009). Interactions of protein molecules with nanoscale surface structures are very important in many research fields, such as biomaterials, biosensors, cell adhesion, biofuel cells and biomineralization. Protein adsorption could be affected by both surface chemical composition and topography. During the past several decades,

Handling Editor: H. S. Sharma.

✉ Ghodratollah Absalan
gubsulun@yahoo.com; absalan@susc.ac.ir

[1] Professor Massoumi Laboratory, Department of Chemistry, College of Science, Shiraz University, 71454 Shiraz, Islamic Republic of Iran

[2] Present Address: Department of Chemistry, Payame Noor University, Tehran, Islamic Republic of Iran

the influence of surface chemical compositions on protein adsorption was extensively studied. One of the most effective and popular approaches is application of hydrophilic polymers such as polyethylene oxide (PEO) onto surfaces (Gonsalves et al. 2005; Chen et al. 2008; Wu et al. 2009).

Lysozyme is a widely distributed enzyme that preferentially hydrolysis β-1,4-glucosidic linkage between *N*-acetylglucosamine and *N*-acetylmuramic acid in bacterial cell walls. Lysozyme has found wide applications; it is often used in conjunction with other therapeutic drugs, applied topically or administered orally (Ghosh and Cui 2000). It has also been used in gastrointestinal infections and in the treatment of dry-mouth (Roy et al. 2003), and food additive in milk products. The potential for its use as an anti-cancer drug has been investigated on animals and in vitro cell culture experiments (Cartei et al. 1991).

The unique physical and chemical characters of ionic liquids (ILs) have made them applicable in diverse chemical areas such as batteries and fuel cells studies (Rezaei et al. 2009), electrochemistry (Heli et al. 2010), chemical synthesis, catalysis (Goharshadi et al. 2009; Valizadeh and Shockravi 2009) and separation sciences (Absalan et al. 2008). They have negligible volatility and non-flammability, wide liquid temperature range, wide electrochemical potential window, high thermal and chemical stability, high solvating capacity for organic, inorganic and organometallic compounds. Their physicochemical properties are finely tunable by altering the cation and/or anion constituents of these molecules (Sun and Armstrong 2010).

The present study focuses on the preparation and characterization of magnetic nanoparticles of Fe_3O_4 modified by different ionic liquids, [C_4MIM][Br], [C_6MIM][Br] and [C_8MIM][Br] by electron microscopy (TEM), X-ray diffraction (XRD), and Fourier transform infrared (FTIR) spectroscopy. The adsorption capacity of Fe_3O_4, [C_4MIM]–Fe_3O_4, [C_6MIM]–Fe_3O_4, and [C_8MIM]–Fe_3O_4 as adsorbents for adsorption of hen egg white lysozyme (LYS) was investigated. Adsorption isotherms, kinetic of adsorption and thermodynamic parameters were also characterized. To the best of our knowledge, adsorption of proteins on magnetic nanoparticles modified with different ionic liquids has not been reported.

Experimental

Apparatus

A UV–Vis. spectrophotometer Model Pharmacia Ultraspec 4000, connected to a personal computer equipped with a 1-cm quartz cell was used for recording the visible spectra and absorbance measurements. The XRD measurements were performed on the XRD Bruker D8 Advance. The FTIR spectra were recorded on a Shimadzu FTIR 8000 spectrometer. A transmission electron microscope (Philips CM 10 TEM) was used for recording of TEM images. A Metrohm 780 pH meter was used for monitoring the pH values. A water ultrasonicator (Model CD-4800, China) was used to disperse the nanoparticles in solution and a super magnet Nd–Fe–B (1.4 T, 10 cm × 5 cm × 2 cm, made in China) was used. All measurements were performed at ambient temperature.

Chemicals and reagents

All chemicals and reagents were of analytical grades. 1-Methylimidazolium, hexyl bromide, butyl bromide, octyl bromide, hen egg white lysozyme (LYS), sodium hydroxide, hydrochloric acid (37 %w/w), sodium thiocyanate, sodium chloride, $FeCl_3.6H_2O$ (96 %w/w) and $FeSO_4.7H_2O$ (99.9 %w/w) were purchased from Merck. The stock solution of protein was prepared with a concentration of 2.0 mg mL^{-1}. The protein solutions with concentrations in the range of 0.05–2.0 mg mL^{-1} were prepared by successive dilution of the stock solution with distilled water. The pH adjustments were performed with HCl and NaOH solutions (0.01–1.0 mol L^{-1}). Ionic liquids, [C_4MIM][Br], [C_6MIM][Br], [C_8MIM][Br] were prepared according to procedure reported in the literature (Bonhote et al. 1996).

Fabrication of ionic liquid modified magnetic nanoparticles

The nanoparticles of Fe_3O_4 were synthesized by mixing ferrous sulfate and ferric chloride in NaOH solution with constant stirring as recommended (Kim et al. 2001). To obtain maximum yield for magnetic nanoparticles during co-precipitation process, the ideal molar ratio of Fe^{2+}/Fe^{3+} was about 0.5. The precipitates were heated at 80 °C for 30 min, sonicated for 20 min, and then washed three times with 50 ml distilled water.

Modification of Fe_3O_4 nanoparticles was carried out using ionic liquids under vigorous magnetic stirring for 30 min at 50 °C. The modified iron oxide nanoparticles (IL–Fe_3O_4) were collected by applying a magnetic field with an intensity of 1.4 T. The IL–Fe_3O_4 particles were washed three times with 50 ml distilled water. Nanoparticles were dispersed in distilled water by ultrasonicating for 10 min at room temperature. Then, the IL–Fe_3O_4 nanoparticles were magnetically separated (Absalan et al. 2011; Ghaemi and Absalan 2014).

Adsorption equilibrium of lysozyme

For adsorption of lysozyme, the modified Fe_3O_4 (40.0 mg) nanoparticles were incubated with 10 ml of the protein

(0.05–2.0 mg mL^{-1}) in 0.1 mol L^{-1} NaCl and the obtained suspension was immediately stirred by a magnetic stirrer (150 rpm) for 10 min. After mixing, the magnet was removed and washed with distilled water. Then the magnetic nanoparticles were removed magnetically from the solution. The lysozyme concentration in the solution was determined by UV spectrophotometry at 280 nm, and the equilibrium adsorption amount was calculated according to Eq. (1).

$$q_e = \frac{V(C_0 - C_e)}{m} \tag{1}$$

where q_e (in mg g^{-1}) is the adsorption capacity (mg lysozyme adsorbed onto gram amount of nanoparticles); V is the volume of the lysozyme solution (in liter); C_0 and C_e are the initial and equilibrium protein concentrations (in mg L^{-1}), respectively; and m is the mass (in gram) of dried IL–Fe_3O_4 added.

Adsorption isotherms

Several isotherm models for evaluating the equilibrium adsorption, have been discussed in literatures (Limousin et al. 2007).

The linear form of the Langmuir isotherm (Langmuir 1918), assuming monolayer adsorption on a homogeneous adsorbent surface, is expressed as:

$$\frac{C_e}{q_e} = \frac{1}{bq\max} + \frac{C_e}{q\max} \tag{2}$$

where q_{max} (mg g^{-1}) is the surface concentration at monolayer coverage and illustrates the maximum value of q_e that can be attained as C_e is increased. The b parameter is a coefficient related to the energy of adsorption and increases with increasing strength of the adsorption bond. Values of q_{max} and b are determined from the linear regression plot of (C_e/q_e) versus C_e.

The Freundlich equation (Freundlich 1906) is expressed in its linear form as follows:

$$\log q_e = \log K_F + \frac{1}{n} \log C_e \tag{3}$$

where K_F and n are the constants from the Freundlich equation representing the capacity of the adsorbent for the adsorbate and the reaction order, respectively. The reciprocal reaction order, $1/n$, is a function of the strength of adsorption.

Adsorption kinetics theory

Several models are available to study the adsorption mechanism and describe the corresponding experimental data. The most commonly models used are the pseudo-first-order and pseudo-second-order reaction rate equations (Santos et al. 2008) developed by Ho and McKay (1999) which have the following linear forms for boundary conditions of $q = 0$ at $t = 0$ and $q_t = q_e$ at $t = t_e$. Pseudo-first-order equation:

$$\frac{dq_t}{dt} = k_1(q_e - q_t) \tag{4}$$

$$\log(q_e - q_t) = \log q_e - k_1 t \tag{5}$$

Pseudo-second-order equation:

$$\frac{dq_t}{dt} = k_2(q_e - q_t)^2 \tag{6}$$

$$\frac{t}{q_t} = \frac{1}{k_2 q_e^2} + \frac{t}{q_e} \tag{7}$$

where k_1 and k_2 are the adsorption rate constants, q_t is adsorption capacity at time t, q_e is adsorption capacity at equilibrium condition.

The structure of the solid and its interaction with the diffusion substance influences the rate of transport. Adsorbent may be in the form of porous barriers and solute moves by diffusion from one fluid body to the other by virtue of concentration gradient. Intra-particle diffusion is a transport process involving movement of species from the bulk of the solution to the solid phase. The intra-particle kinetic model is expressed by:

$$Q_t = k_i t^{1/2} + C \tag{8}$$

Results and discussion

Characterization of Fe_3O_4 and IL–Fe_3O_4

The peaks positions and relative intensities observed in XRD patterns of IL–Fe_3O_4 ([C_4MIM]–Fe_3O_4, [C_6MIM]–Fe_3O_4, [C_8MIM]–Fe_3O_4) nanoparticles and standard Fe_3O_4 are shown in Fig. 1 for comparison. Although the magnetic nanoparticle surfaces in IL–Fe_3O_4 were coated with ionic liquid, analysis of XRD patterns of Fe_3O_4, [C_4MIM]–Fe_3O_4, [C_6MIM]–Fe_3O_4 and [C_8MIM]–Fe_3O_4 indicated very distinguishable peaks for magnetite crystal, which means that these particles have phase stability (Park et al. 2008; Faivre and Zuddas 2006).

The FTIR spectra of Fe_3O_4, ionic liquid and IL–Fe_3O_4 are shown in Fig. 2a–c. In the case of Fe_3O_4, the broad absorption band at 3440 cm^{-1} indicates the presence of surface hydroxyl groups (O–H stretching) and the bands at low wavenumbers ($\leq$700 cm^{-1}) are related to vibrations of the Fe–O bonds in iron oxide. The presence of magnetite nanoparticles can be verified by appearance of two strong absorption bands around 632 and 585 cm^{-1} (Waldron 1955; Can et al. 2009). The Fe–O bond peak of the

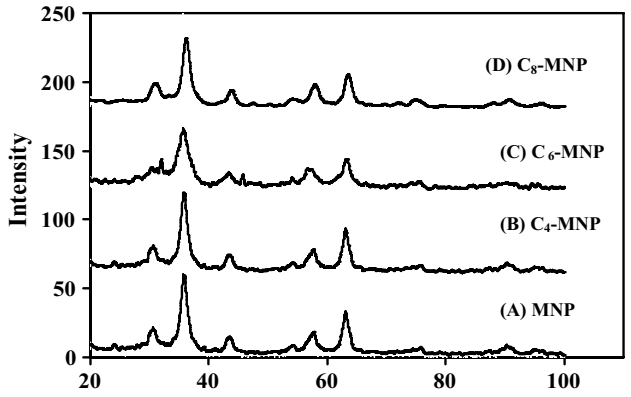

Fig. 1 The XRD pattern of: Fe_3O_4 (*A*), [C_4MIM]–Fe_3O_4 (*B*), [C_6MIM]–Fe_3O_4 (*C*), [C_8MIM]–Fe_3O_4 (*D*)

bulk magnetite is observed at 570.9 cm^{-1}. In the spectrum of ionic liquids (Fig. 2a–c), a long hydrocarbon chain in [C_4MIM][Br], [C_6MIM][Br] and [C_8MIM][Br] gives significantly stronger peaks in the ranges of 2800–3100 and 1465–1640 cm^{-1}. In the FTIR spectra of [C_6MIM]-Fe_3O_4 and [C_8MIM]-Fe_3O_4, the significant absorption band, respectively, at 2923.9 and 2931.6 cm^{-1} is due to the C–H stretching. This band was not observed in the spectrum of [C_4MIM]–Fe_3O_4. The absorption bands indicating the C–N stretching are observed at 1542.9, 1447.5 and 1458.1 cm^{-1}, respectively, for [C_4MIM]–Fe_3O_4, [C_6MIM]–Fe_3O_4, and [C_8MIM]–Fe_3O_4. The absorption bands at 1612.4, 1604.0 and 1627.8 cm^{-1} are related to the hetro-aromatic C–H bond stretching for [C_4MIM]–Fe_3O_4, [C_6MIM]–Fe_3O_4, [C_8MIM]–Fe_3O_4, respectively.

Figure 3a is a representative TEM image of Fe_3O_4 nanoparticles. The average diameter of Fe_3O_4 nanoparticles was about ~10 nm. However, the TEM image, as shown in Fig. 3 (b–d) indicated that IL–Fe_3O_4 (13–15 nm) had a larger particle diameter than Fe_3O_4.

It is known that when an electrolyte is added to a colloidal aqueous solution, it reduces the surface charges of these particles and causes their agglomeration. Similarly, ionic liquids are expected to reduce the surface charges of nanoparticles. If we assume that the difference of 3–5 nm in the mean sizes of modified and unmodified nanoparticles is significant, it reveals that ionic liquids have reduced the surface charges of Fe_3O_4 nanoparticles and caused their agglomeration.

To estimate the amount of ionic liquid deposited onto the surface of Fe_3O_4, the thermogravimetric analysis (TGA) of Fe_3O_4 and IL–Fe_3O_4 was conducted. Figure 4 shows the TGA curves of Fe_3O_4, [C_4MIM]–Fe_3O_4, [C_6MIM]–Fe_3O_4, and [C_8MIM]–Fe_3O_4 nanoparticles. For [C_4MIM]–Fe_3O_4 and [C_6MIM]–Fe_3O_4 in the lower temperature range (up to 201 °C), the initial weight loss was not observed but initial

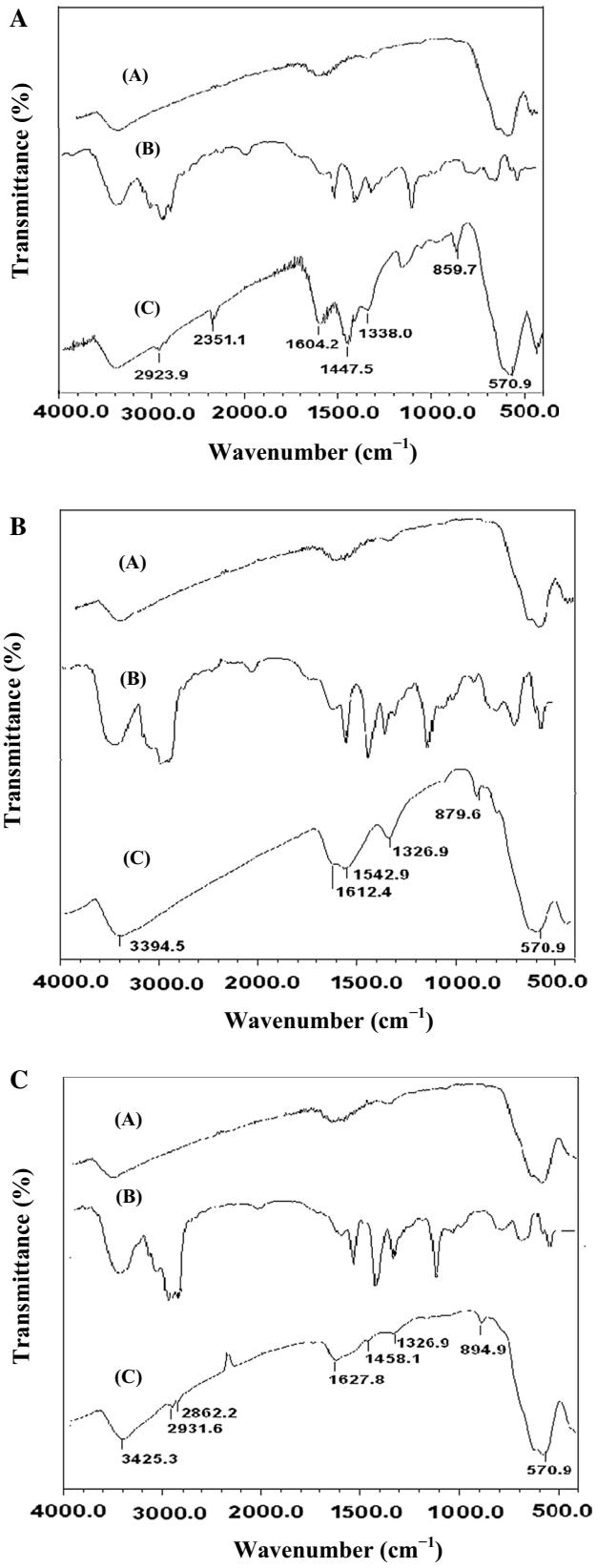

Fig. 2 **a** The FTIR spectra of: Fe_3O_4 (*A*), [C_6MIM] [Br] (*B*) and [C_6MIM]–Fe_3O_4 (*C*). **b** The FTIR spectra of: Fe_3O_4 (*A*), [C_4MIM] [Br] (*B*) and [C_4MIM]–Fe_3O_4 (*C*). **c** The FTIR spectra of: Fe_3O_4, (*A*), [C_8MIM][Br] (*B*), and [C_8MIM]–Fe_3O_4 (*C*)

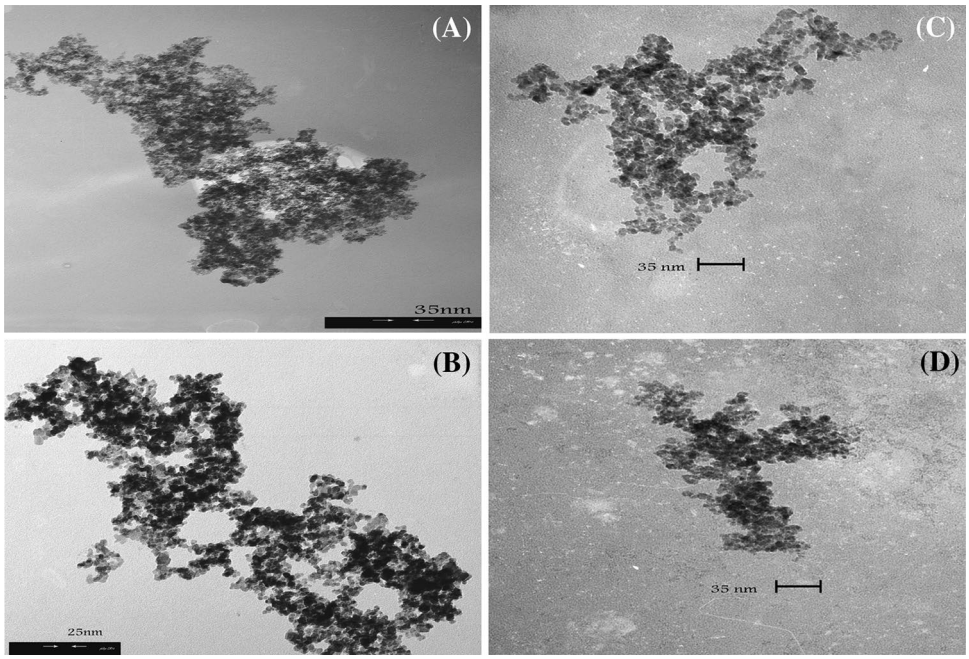

Fig. 3 The TEM images of: Fe_3O_4 (*A*), [C_6MIM]–Fe_3O_4 (*B*), [C_4MIM]–Fe_3O_4 (*C*), and [C_8MIM]–Fe_3O_4 (*D*)

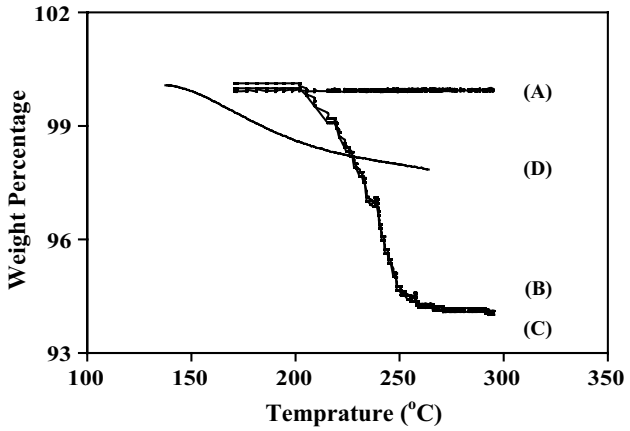

Fig. 4 The TGA graphs of: Fe_3O_4 (*A*), [C_4MIM]–Fe_3O_4 (*B*), [C_6MIM]–Fe_3O_4 (*C*), and [C_8MIM]–Fe_3O_4 (*D*)

weight loss was from 145 °C for C_8MIM]–Fe_3O_4 nanoparticles. The weight loss of both [C_4MIM]–Fe_3O_4 and [C_6MIM]–Fe_3O_4 nanoparticles occurred in the temperature range of 201–261 °C which was due to the decomposition of ionic liquid. At temperatures above 261 °C, the ionic liquid was completely decomposed. The residual weight should be the weight of Fe_3O_4. According to the TGA curves, the ionic liquid content of [C_4MIM]–Fe_3O_4 and [C_6MIM]–Fe_3O_4 nanoparticles was evaluated to be 5.82 % by weight. But the ionic liquid content of [C_8MIM]–Fe_3O_4 nanoparticles was 2.15 % by weight. The loading of [C_8MIM][Br] onto the surfaces of Fe_3O_4 nanoparticles is limited due to the long hydrocarbon chains of its molecules where cause steric hindrance for each other.

The experimental curves corresponding to the immersion technique (Foil and Villaescusa 2009; Uddin et al. 2009) were obtained for four sorbents and are presented in Fig. 5. Suspensions of 5.5 g L^{-1} of individual sorbents were prepared and were put into contact with 0.10 mol L^{-1} of NaCl solutions adjusted at different pH values. The aqueous suspensions were agitated for 48 h until the equilibrium pH was achieved. The pH value at the point of zero charge (pH_{pzc}) was determined by plotting the difference of final and initial pHs (ΔpH) versus the initial pH. As shown in Fig. 5, the pH_{pzc} value of Fe_3O_4 is 6.5 and the pH_{pzc} values for [C_4MIM]–Fe_3O_4, [C_6MIM]–Fe_3O_4 and [C_8MIM]–Fe_3O_4 nanoparticles are 8.0, which means that the pH of Fe_3O_4 has shifted from 6.5 to 8.0 after modification with ionic liquid. This confirmed the deposition of ionic liquid onto the surface of Fe_3O_4 and also revealed that IL–Fe_3O_4 was positively charged at pH < 8.0.

The adsorption isotherm of IL ([C_{16}MIM]Br and [C_{10}MIM]Br) onto Fe_3O_4 at pH 10 was already reported (Zhang et al. 2010). Adsorption could be considered as hemimicelles formation in which IL molecules were adsorbed on the oppositely charged Fe_3O_4 nanoparticles surface to form single layer coverage through coulombic attraction interaction.

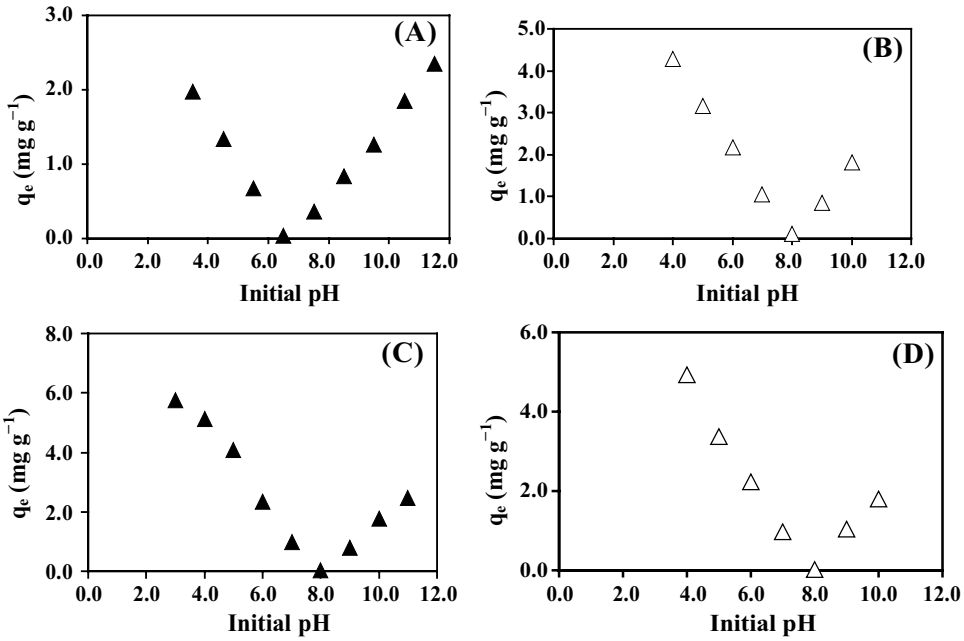

Fig. 5 Immersion technique curve of Fe_3O_4, (*A*); [C_4MIM]–Fe_3O_4, (*B*); [C_6MIM]–Fe_3O_4, (*C*); and [C_8MIM]–Fe_3O_4,(*D*)

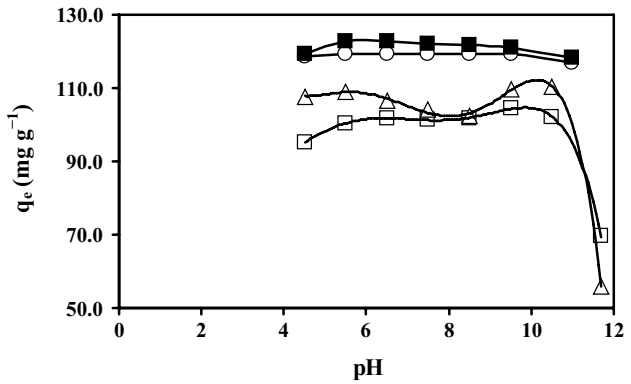

Fig. 6 Effect of initial pH solution on adsorption of lysozyme onto: unmodified–Fe_3O_4 (*unfilled triangle*), [C_4MIM]–Fe_3O_4 (*unfilled square*), [C_6MIM]–Fe_3O_4 (*filled square*), and [C_8MIM]–Fe_3O_4 (*unfilled circle*). Experimental conditions: nanoparticles dosage of 40.0 mg, initial lysozyme concentration of 0.5 mg mL^{-1}, stirring time of 5 min

Adsorption of lysozyme on modified nanoparticles

Effect of pH

The effect of the initial pH of the sample solution on the adsorption of LYS onto four modified nanoparticles was assessed at different pH values, ranging from 3.5 to 11.0. The initial concentration of LYS and adsorbent dosage were set at 0.5 mg mL^{-1} and 40.0 mg, respectively. The LYS solution was stirred for a period of 5 min while the experiments were performed in batch technique. The results are depicted in Fig. 6. At pH values below 9.5, almost a constant and high value for adsorption capacity of each adsorbent was observed. At pH values higher than 9.5, adsorption of LYS is decreased probably due to instability of the modified nanoparticles at high hydroxyl ion concentration that consequently result in reduction of the adsorption of LYS onto nanoparticles.

Adsorption capacity of both [C_6MIM]–Fe_3O_4 and [C_8MIM]–Fe_3O_4 is higher than [C_4MIM]–Fe_3O_4 and unmodified–Fe_3O_4. This could be explained based on the hydrophobic characters of ILs. The hydrophobic characters of [C_6MIM][Br] and [C_8MIM][Br] are higher than [C_4MIM][Br] due to the length of the hydrocarbon chain (Rıos et al. 2008).

Effect of contact time

The effects of stirring time on the adsorption of lysozyme onto four nanoparticles were studied individually. IL–Fe_3O_4 of 40.0 mg and optimum pH of 9.0 were considered for this investigation. The initial lysozyme concentrations for all test solutions were 0.5 mg mL^{-1}. Figure 7 shows adsorption capacity for three adsorbents as a function of stirring time ranging from 1 to 16 min. These data indicate that adsorption process is almost completed within 5 min. The initial slopes of the curves in Fig. 7 show that the rate of adsorption of LYS onto the unmodified nanoparticles is the slowest among the other adsorbents; the rates of LYS adsorption onto modified nanoparticles are almost the same which shows that the kinetic of adsorption is independent of the type of the ionic liquids used as modifiers. Moreover, the adsorption efficiency was increased when the ionic liquids were used as modifier. Amongst them, [C_6MIM]–Fe_3O_4 and [C_8MIM]–Fe_3O_4 showed higher efficiencies.

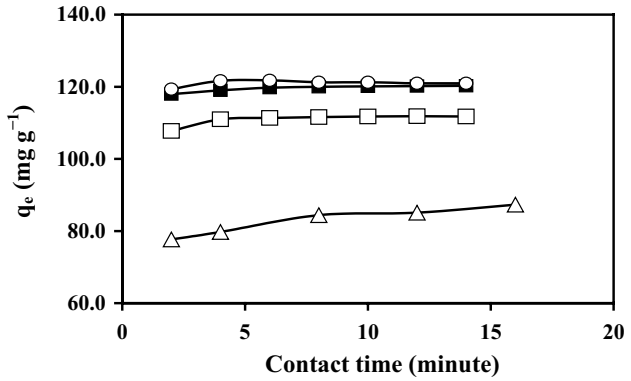

Fig. 7 Effect of stirring time on adsorption of lysozyme onto unmodified Fe_3O_4 (*unfilled triangle*), [C_4MIM]–Fe_3O_4 (*unfilled square*), [C_6MIM]–Fe_3O_4, (*filled square*); and [C_8MIM]–Fe_3O_4 (*unfilled circle*). Experimental conditions: nanoparticles dosage of 40.0 mg, initial lysozyme concentration of 0.5 mg mL^{-1} at the pH 9.0

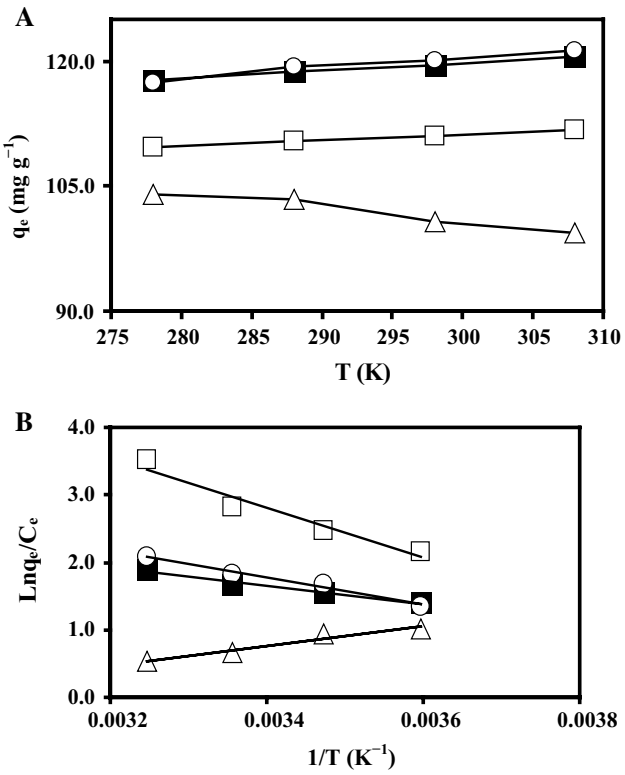

Fig. 8 **a** Effect of temperature. **b** The plots of ln (qe/Ce) against 1/T for adsorption of lysozyme onto unmodified Fe_3O_4 (*unfilled triangle*), [C_4MIM]–Fe_3O_4 (*unfilled square*), [C_6MIM]–Fe_3O_4 (*filled square*), and [C_8MIM]–Fe_3O_4 (*filled circle*). Experimental conditions: nanoparticles dosage of 40.0 mg, initial lysozyme concentration of 0.5 mg mL^{-1}, stirring time of 10 min at pH 9.0

Effect of solution temperature

The effect of temperature on the adsorptions of LYS onto four nanoparticles was investigated at optimum pH and initial protein concentrations of 0.5 mg mL^{-1} with a stirring time of 10 min. Figure 8 shows adsorption capacity of lysozyme for four adsorbents as a function of temperature ranging between 278 and 308 K. The results indicate that the solution temperature strongly affected the adsorption capacity of LYS. For all IL–Fe_3O_4 nanoparticles, adsorption capacity increases with increasing temperature indicating the endothermic ($\Delta H > 0$) nature of the adsorption process.

The results indicate that the adsorption capacity of unmodified Fe_3O_4 for LYS decreased with increasing temperature in the applied temperature range of 278–308 K. So, the adsorption of LYS onto unmodified Fe_3O_4 is concluded to be exothermic ($\Delta H_{\text{unmodified}} < 0$), i.e., higher adsorption can be obtained at lower temperatures. The value of $\Delta H_{\text{unmodified}}$ includes three terms, dehydration enthalpy, ΔH_d (endothermic); adsorption affinity enthalpy, ΔH_a (exothermic); and molecular conformation enthalpy, ΔH_m (exothermic). Therefore, the exothermic effect of $\Delta H_{\text{unmodified}}$ must be attributed to both ΔH_a and ΔH_m as their summation predominates over ΔH_d so that the net enthalpy would be negative in sign. Similarly, the value of $\Delta S_{\text{unmodified}}$ includes three terms, dehydration entropy, ΔS_d; adsorption affinity entropy, ΔS_a; and molecular conformation entropy, ΔS_m. The value of $\Delta S_{\text{unmodified}}$ is negative due to ΔS_a and ΔS_m as their summation predominates over ΔS_d (Geng et al. 2008). Since $T\Delta S_{\text{unmodified}}$ is more positive than $\Delta H_{\text{unmodified}}$, the mathematical sign of $\Delta G_{\text{unmodified}}$ is positive.

The plot of ln (q_e/C_e) versus $1/T$ is indicated in the inset of Fig. 8. From the slope and intercept, the changes of enthalpy (ΔH) and entropy (ΔS) at 278–308 K could be determined. Table 1 shows thermodynamic parameters of adsorption for LYS onto nanoparticles. The free energy of the adsorption processes for LYS onto IL–Fe_3O_4 at all temperatures was almost negative indicating the feasibility of the process and the spontaneous nature of the adsorption. The negative ΔG value increased with increasing temperature, indicating that the spontaneity adsorption is proportional to the temperature. According to data in Table 1, electrostatic interactions between adsorbate and adsorbent were not significant in the temperature range of 278–308 K; it is considerable in higher temperature range.

The positive values of ΔH, Table 1, indicate that adsorption of lysozyme onto IL–Fe_3O_4 is endothermic, i.e., better adsorption can be obtained at higher temperatures. In contrast to the case of the unmodified nanoparticles, the endothermic adsorption process of LYS onto modified nanoparticles must be attributed to the dehydration processes, i.e., ΔH_d predominates over ΔH_a and ΔH_m so that the net enthalpy (ΔH) is positive in sign. The positive sign of ΔS for adsorption process of LYS onto modified nanoparticles indicates that dehydration entropy must predominate (Geng

Table 1 Thermodynamic parameters of adsorption of lysozyme onto unmodified and modified Fe_3O_4 nanoparticles

Adsorbent	ΔS_0^T (J mol^{-1} K^{-1})	ΔH_0^T (kJ mol^{-1})	ΔG_0^T (kJ mol^{-1})			
			278 K	288 K	298 K	308 K
Fe_3O_4	−35.54	−12.31	2.43	2.07	1.72	1.36
[C_4MIM]–Fe_3O_4	128.60	30.96	−4.79	−6.08	−7.38	−8.65
[C_6MIM]–Fe_3O_4	52.79	11.47	−3.21	−3.73	−4.26	−4.79
[C_8MIM]–Fe_3O_4	71.07	16.57	−3.18	−3.89	−4.60	−5.31

Table 2 Adsorption isotherms parameters of lysozyme onto Fe_3O_4 and modified Fe_3O_4 nanoparticles

Adsorbent	Langmuir model			Freundlich model		
	q_{max} (mg g^{-1})	b (L mg^{-1})	R^2	K_F (mg g^{-1})	n (g L^{-1})	R^2
Fe_3O_4	370.4	0.004	0.938	5.48	1.59	0.912
[C_4MIM]–Fe_3O_4	400.0	0.019	0.995	23.35	2.02	0.946
[C_6MIM]–Fe_3O_4	500.0	0.024	0.961	24.74	1.70	0.777
[C_8MIM]–Fe_3O_4	526.3	0.012	0.849	29.09	2.12	0.573

et al. 2008). As a result, the thermodynamic data indicate that the adsorption process of LYS onto the modified nanoparticles is entropy driven.

Effect of lysozyme concentration

The initial lysozyme concentration is another factor that can affect its adsorption process. Different concentrations of LYS were studied for their adsorption onto four different types of nanoparticles under previously determined optimum experimental conditions. The results, in terms of adsorption capacity versus initial concentration of LYS, are indicated such that adsorption capacity of lysozyme increased when Fe_3O_4 nanoparticles were modified by ionic liquids. Adsorption capacity of lysozyme onto IL–Fe_3O_4 depends on the hydrophobic character of the ionic liquid, i.e., an ionic liquid with a high length of the hydrocarbon chain presents the highest adsorption capacity (Rıos et al. 2008). The order of hydrophobicity of the ionic liquids is [C_8MIM][Br] > [C_6MIM][Br] > [C_4MIM][Br].

Adsorption isotherm modeling

The equilibrium adsorption data of LYS on four types of nanoparticles were analyzed using Langmuir and Freundlich models. Model fitting to equilibrium adsorption results of LYS were assessed based on the values of the correlation coefficient (R^2) of the linear regression plot. The experimental data were checked for their probable fitting to both models. Table 2 summarizes the models constants and the corresponding correlation coefficients. As shown in Table 2, the R^2 value for the Langmuir isotherm was higher than that of the Freundlich isotherm for the adsorption of LYS onto four adsorbents. This indicates that the adsorptions of LYS onto all applied nanoparticles are better described by the Langmuir model than the Freundlich model. According to the Langmuir model, monolayer adsorption of adsorbate occurs onto the surface of the adsorbent (Langmuir 1918). Table 2 shows that the maximum adsorption capacity for LYS onto Fe_3O_4, [C_4MIM]–Fe_3O_4, [C_6MIM]–Fe_3O_4 and [C_8MIM]–Fe_3O_4 nanoparticles are 370, 400, 500 and 526 mg g^{-1}, respectively. It should be mentioned that the lysozyme adsorption process is affected by the chemical and physical properties of the adsorbents, particularly by the difference in the charge density and hydrophobicity of the ionic liquids as modifier. As seen in Table 2, the adsorption capacity of the IL-modified magnetic nanoparticles for adsorption of LYS increases by using ionic liquids in the order of [C_8MIM][Br] > [C_6MIM][Br] > [C_4MIM][Br], this corresponds to the order of hydrophobicity of the ionic liquid. These results are in agreement with those reported in the literatures (Rıos et al. 2008; Ropel et al. 2005). This shows that the hydrophobicity of the modifiers is an important factor to be considered for increasing the adsorption capacity of the magnetic nanoparticles. It is noticeable that the hydrophobicity of an ionic liquid in majority is determined by the nature of its cationic constituent.

Adsorption kinetic modeling

Different kinetic parameters of LYS adsorption onto four adsorbents for LYS initial concentration of 0.5 mg mL^{-1} are shown in Table 3. All experimental data showed better agreement with pseudo-second-order kinetic model in terms of higher correlation coefficient values ($R^2 \approx 1$). Corresponding to kinetic parameters reported in Table 3,

Table 3 Adsorption kinetic constants of Lysozyme onto Fe_3O_4 and modified Fe_3O_4 nanoparticles

Adsorbent	Pseudo-first-order model			Pseudo-second-order model			Intra-particle diffusion		
	k_1 (min^{-1})	q_e (mg g^{-1})	R^2	k_2 (g $mg^{-1}min^{-1}$)	q_e (mg g^{-1})	R^2	k_i ($gmg^{-1}min^{-1}$)	C (mg g^{-1})	R^2
Fe_3O_4	0.089	15.55	0.9683	0.039	87.0	0.9998	4.83	70.56	0.986
$[C_4MIM]$–Fe_3O_4	0.454	7.71	0.967	0.132	112.4	1.0	0.65	109.72	0.993
$[C_6MIM]$–Fe_3O_4	0.092	1.68	0.9557	0.172	120.5	1.0	1.73	115.5	0.998
$[C_8MIM]$–Fe_3O_4	0.209	1.182	0.2551	0.672	122.0	1.0	2.42	116.19	0.870

modification of Fe_3O_4 nanoparticles by ionic liquid could cause decrease in contact time.

Intra-particle diffusion (Kamran et al. 2014) is a transport process involving movement of species from the bulk of the solution to the solid phase surface. The mechanism for adsorption of a protein on nanoparticles is assumed as a three-step process in which bulk diffusion, i.e., migration of the protein from the bulk of the solution to the boundary layer nearby the surface of the nanoparticle, is not considered. The first step is diffusion of protein through the boundary layer towards the surface of the adsorbent. The second step is the protein transfer from the exterior surface of the adsorbent particle to the interior pores of the particle through a pore diffusion or intra-particle diffusion mechanism. Finally, the adsorption occurs onto an active site of adsorbent via an ion exchange and/or a complexation process (Yang et al. 2011; Kamran et al. 2013; Elass et al. 2011). According to intra-particle diffusion model, the plot of uptake should be linear if intra-particle diffusion is involved in an adsorption process. If this line passes through the origin then intra-particle diffusion is the rate-controlling step. When the plot does not pass through the origin, this is indicative of some degree of boundary layer control. This shows that the intra-particle diffusion is not the only rate limiting step, but also other kinetic models may control the rate of adsorption, all of which may be operating simultaneously (Gusmãoa et al. 2012). According to the intra-particle diffusion model, the slope of the linearized plot characterizes the rate parameter of the diffusion, whereas the intercept is proportional to the boundary layer thickness. In this study, the correlation coefficient (R^2) value of the model indicates the possibility of intra-particle diffusion (Table 3) for the protein adsorbed onto magnetic nanoparticles.

Desorption and reusability studies

For potential applications, regeneration and reusability of an adsorbent are important factors to be reported. Possible desorption of LYS was tested by using different solutions such as sodium chloride solution (1.0 mol L^{-1}) and sodium thiocyanate solution (1.0 mol L^{-1}); both were tested at pH 9.5 and 11.0. This study revealed that the adsorbed LYS could be quantitatively desorbed in the presence of either NaCl or thiocyanate at pH 9.5. After adsorption of LYS from 10 mL of its 0.5 mg mL^{-1} solution onto 40 mg IL–Fe_3O_4 nanoparticles, about 96–98 % of LYS was desorbed (recovered) by 10 ml of 1.0 mol L^{-1} solution of either sodium chloride or thiocyanate at pH 9.5 within 20 and 10 min, respectively. The results showed that a three-consecutive desorbing process can improve the desorption process. By adding NaCl, the ionic strength is increased and consequently, the electrostatic and/or hydrophobic attraction between LYS and IL–Fe_3O_4 nanoparticles is reduced such that in turn provides a feasible desorption process. A much faster desorption process was observed in the presence of NaSCN not only due to increase of ionic strength but also due to the fact that SCN^- ions are easily bonded to protein molecules (Zhang et al. 2006). It should be mentioned that no change in color of the solution due to possible formation of red-color $FeSCN^{2+}$ ions was observed proving that the IL–Fe_3O_4 nanoparticles were undamaged in this process.

The reusability of the adsorbents in several successive separation processes was tested and the result showed that IL–Fe_3O_4 can be reused for three times without significant reduction in its adsorption capacity.

Conclusions

The IL–Fe_3O_4 nanoparticles were quite efficient as magnetic nano-adsorbents for fast adsorbing of LYS from aqueous solutions. The time required to achieve the adsorption equilibrium was 10 min. The adsorption of LYS onto the surface of three types of IL–Fe_3O_4 nanoparticles was concluded to be attributed to the surface electrostatic and hydrophobic interactions between protein and IL–Fe_3O_4 nanoparticles. The adsorption data followed the Langmuir isotherm equation. The maximum adsorption capacities for LYS onto Fe_3O_4, $[C_4MIM]$–Fe_3O_4, $[C_6MIM]$–Fe_3O_4 and $[C_8MIM]$–Fe_3O_4 were 370.0, 400.0, 500.0, and 526.3 mg g^{-1}, respectively. The Langmuir adsorption constants for adsorption of LYS onto Fe_3O_4, $[C_4MIM]$–Fe_3O_4, $[C_6MIM]$–Fe_3O_4 and $[C_8MIM]$–Fe_3O_4 were 0.004, 0.019, 0.024 and 0.012 L mg^{-1}, respectively. The enthalpy change

of adsorptions were found to be −12.31, 30.96, 11.47 and 16.57 kJ mol^{-1} when Fe_3O_4, $[C_4MIM]$–Fe_3O_4, $[C_6MIM]$–Fe_3O_4 and $[C_8MIM]$–Fe_3O_4, respectively, were used as adsorbents for LYS. Kinetic data were appropriately fitted to pseudo-second-order adsorption rates. The NaCl solution at pH 9.5 was suitable for desorbing LYS and the recycled IL–Fe_3O_4 was usable for three times.

Acknowledgments The authors wish to acknowledge the support of this work by Shiraz University Research Council. Dr. M. M. Doroodmand for TGA, Department of Physics for XRD and Veterinary Faculty for TEM are acknowledged.

Compliance with ethical standards

Conflict of interest We have no potential conflict of interest.

References

Absalan G, Akhond M, Sheikhian L (2008) Extraction and high performance liquid chromatographic determination of 3-indole butyric acid in pea plants by using imidazolium-based ionic liquids as extractant. Talanta 77:407–411

Absalan G, Asadi M, Kamran S, Sheikhian L, Goltz DM (2011) Removal of reactive red-120 and 4-(2-pyridylazo) resorcinol from aqueous samples by Fe3O4 magnetic nanoparticles using ionic liquid as modifier. J Hazard Mater 192:476–484

Altıntas EB, Denizli A (2009) Monosize magnetic hydrophobic beads for lysozyme purification under magnetic field. Mater Sci Eng C 29:1627–1634

Bonhote P, Dias AP, Papageorgion N, Kalyanasundaran K, Gratzel M (1996) highly conductive ambient-temperature molten salts. Inorg Chem 35:1168–1178

Can K, Ozmen M, Ersoz M (2009) Immobilization of albumin on aminosilane modified superparamagnetic magnetite nanoparticles and its characterization. Colloids Surf B Biointerfaces 71:154–159

Cartei F, Cartei G, Ceschia V, Pacor S, Sava G (1991) Hematologic effects of oral treatment with lysozyme chloride: a phase-II study. Curr Therap Res Clin Exp 50:530–538

Chen X, Wu T, Wang Q, Shen JW (2008) Shield effect of silicate on adsorption of proteins onto silicon-doped hydroxyapatite (100) surface. Biomaterials 29:2423–2432

Elass K, Laachach A, Alaoui A (2011) Azzi M, Removal of methyl violet from aqueous solution using a stevensite-rich clay from Morocco. Appl Clay Sci 54:90–96

Faivre D, Zuddas P (2006) An integrated approach for determining the origin of magnetite nanoparticles. Earth Planet Sci Lett 243:53–60

Foil N, Villaescusa I (2009) Determination of sorbent point zero charge: usefulness in sorption studies. Environ Chem Lett 7:79–84

Freundlich HMF (1906) Over the adsorption in solution. J Phys Chem 57:385–471

Geng XP, Zheng MR, Wang BH, Lei ZM, Geng XD (2008) Fractions of thermodynamic functions for native lysozyme adsorption onto moderately hydrophobic surface. J Therm Anal Calorim 93:503–508

Ghaemi M, Absalan G (2014) Study on the adsorption of DNA on Fe3O4 nanoparticles and on ionic liquid-modified Fe3O4 nanoparticles. Microchim Acta 181:45–53

Ghali M (2010) Static quenching of bovine serum albumin conjugated with small size CdS nanocrystalline quantum dots. J Lumin 130:1254–1257

Ghosh R, Cui ZF (2000) Protein purification by ultrafiltration with pretreated membrane. J Membr Sci 167:47–53

Goharshadi EK, Ding Y, Jorabchi MN, Nancarrow P (2009) Ultrasound-assisted green synthesis of nanocrystalline ZnO in the ionic liquid [hmim][NTf2]. Ultrason Sonochem 16:120–123

Gonsalves IC, Martins MCL, Barbosa MA, Ratner BD (2005) Protein adsorption on 18-alkyl chains immobilized on hydroxyl-terminated self-assembled monolayers. Biomaterials 26:3891–3899

Gupta PK, Hung CT, Lam FC, Perrier DG (1988) Albumin microspheres (III) Synthesis and characterization of microspheres containing adriamycin and magnetite. Int J Pharm 43:167–177

Gusmãoa KAG, Gurgel LVA, Meloa TMS, Gil LF (2012) Application of succinylated sugarcane bagasse as adsorbent to remove methylene blue and gentian violet from aqueous solutions-Kinetic and equilibrium studies. Dyes Pigm 92:967–974

Heli H, Majdi S, Jabbari A, Sattarahmady N, Moosavi-Movahedi AA (2010) Electrooxidation of dextromethorphan on a carbon nanotube–carbon microparticle–ionic liquid composite: applied to determination in pharmaceutical forms. J Solid State Electrochem 14:1515–1523

Ho YS, McKay G (1999) Pseudo-second-order model for sorption processes. Process Biochem 34:451–465

Kamran S, Asadi M, Absalan G (2013) Adsorption of acidic, basic, and neutral proteins from aqueous samples using Fe3O4 magnetic nanoparticles modified with an ionic liquid. Microchim Acta 108:41–48

Kamran S, Asadi M, Absalan G (2014) Adsorption of folic acid, riboflavin, and ascorbic acid from aqueous samples by Fe3O4 magnetic nanoparticles using ionic liquid as modifier. Anal Methods 6:798–806

Kim DK, Zhang Y, Voit W, Rao KV, Muhammed M (2001) Synthesis and characterization of surfactant-coated superparamagnetic monodispersed iron oxide nanoparticles. J Magn Magn Mater 225:30–36

Langmuir I (1918) The adsorption of gases on plane surfaces of glass, mica and platinum. J Am Chem Soc 40:1361–1403

Li ZP, Li KA, Tong SY (1998) Microdetermination of protein with the 1.10-phenanthroline-H2O2-cetyltrimethylammonium bromide-Cu(II) chemiluminescence system. Microchem J 60:217–223

Limousin G, Gaudet P, Charlet L, Szenknect S, Barthés V, Krimissa M (2007) Sorption Isotherms: a review on physical bases, modeling and measurement. Appl Geochem 22:249–275

Miao-Miao T, Ri-Yan S, Qiong J, Chang-Li B, Xin-Jun Q (2011) Spectro-photometric determination of Lysozyme by On-line Preconcentration with a microcolumn containing La3+ -TiO2-Zeolite. Chin J Anal Chem 39:103–106

Mornet S, Vasseur S, Grasset F, Duguet E (2004) Magnetic nanoparticle design for medical diagnosis and therapy. J Mater Chem 14:2161–2175

Murray CB, Kagan JR, Wendi MG (1995) Self-organization of CdSe nanocrystallites into three-dimensional quantum dot superlattices. Science 270:1335–1338

Parhi P, Golas A, Barnthip N, Noh H, Vogler EA (2009) Volumetric interpretation of protein adsorption: capacity scaling with adsorbate molecular weight and adsorbent surface energy. Biomaterials 30:6814–6824

Park SI, Kim JH, Lim JH, Kim CO (2008) Surface-modified magnetic nanoparticles with lecithin for applications in biomedicine. Curr Appl Phys 8:706–709

Rezaei B, Mallakpour S, Taki M (2009) Application of ionic liquids as an electrolyte additive on the electrochemical behavior of lead acid battery. J Power Sources 187:605–612

Rıos PDL, Fernandez FJH, Francisca TA, Manuel R, Demetrio G, Gloria V (2008) On the importance of the nature of the ionic liquids in the selective simultaneous separation of the substrates and products of a transesterification reaction through supported ionic liquid membranes. J Mem Sci 307:233–238

Roath S (1993) Biological and biomedical aspects of magnetic fluid technology. J Magn Magn Mater 122:329–334

Ropel L, Belveze LS, Aki SNVK, Stadtherr MA, Brennecke JF (2005) Octanol–water partition coefficients of imidazolium-based ionic liquids. Green Chem 7:83–90

Roy I, Rao MVS, Gupta MN (2003) Purification of lysozyme from other hen's-egg-white proteins using metal-affinity precipitation. Biotechnol Appl Biochem 37:9–14

Santos SCR, Vilar VJP, Boaventura RAF (2008) Waste metal hydroxide sludge as adsorbent for a reactive dye. J Hazard Mater 153:999–1008

Sun P, Armstrong DW (2010) Ionic liquids in analytical chemistry. Anal Chim Acta 661:1–16

Uddin MT, Islam MA, Mahmud S, Rukanuzzaman M (2009) Adsorptive of removal of methylene blue by tea waste. J Hazard Mater 164:53–60

Valizadeh H, Shockravi A (2009) Imidazolium-based phosphinite ionic liquid as reusable catalyst and solvent for one-pot synthesis of 3,4-dihydropyrimidin-2(1H)- (thio)ones. Heteroat Chem 20:284–288

Waldron RD (1955) Infrared spectra of ferrites. Phys Rev 99:1727–1735

Widder K, Flouret G, Senyei A (1979) Magnetic microspheres: synthesis of a novel parenteral drug carrier. J Pharm Sci 68:79–82

Wu ZQ, Chen H, Liu XL, Zhang YX, Li D, Huang H (2009) Protein adsorption on poly(N-vinylpyrrolidone)-modified silicon surfaces prepared by surface-initiated atom transfer radical polymerization. Langmuir 25:2900–2906

Yang Y, Jin D, Wang G, Liu D, Jia X, Zhao Y (2011) Biosorption of Acid Blue 25 by unmodified and CPC-modified biomass of Penicillium YW01: kinetic study, equilibrium isotherm and FTIR analysis. Colloids Surf B 88:521–526

Zhang J, Zhang Z, Song Y, Cai H (2006) Bovine serum albumin (BSA) adsorption with Cibacron Blue F3GA attached chitosan microspheres. React Funct Polym 66:916–923

Zhang Q, Tang F, Zeng K, Wu K, Cai Q, Yao S (2010) Ionic liquid-coated Fe3O4 magnetic nanoparticles as an adsorbent of mixed hemimicelles solid-phase extraction for preconcentration of polycyclic aromatic hydrocarbons in environmental samples. Analyst 135:2426–2433